

## DEMAGNETIZING FIELD COMPUTATION FOR DYNAMIC SIMULATION OF THE MAGNETIZATION REVERSAL PROCESS

M. Mansuripur and R. Giles, Boston University, Boston, Massachusetts 02215

### ABSTRACT

The magnetic field distribution for a thin magnetic film is computed using the fast Fourier transform technique. The method is quite general and accommodates any 2-dimensional magnetization distribution. It allows the computation of fields both inside the film (demagnetizing fields) and outside (stray fields and leakage).

### Introduction

Computer simulation of magnetization dynamics in thin films is a valuable tool in the analysis of magnetic, bubble, and magneto-optic storage devices. With the advent of powerful computers in recent years, there has been a flurry of activity in micromagnetics research based on computer simulations of the Landau-Lifshitz-Gilbert equation [1]-[4]. The computation-intensive part of these simulations turns out to be the calculation of demagnetizing forces which are rooted in long range dipole-dipole interactions. Truncating the interaction range is not admissible in three-dimensional problems and in two dimensions serious inaccuracies may result unless the truncated terms are sufficiently far away. Another problem is the inherent inaccuracy of straight-forward discretization: Replacing the magnetization within a unit cell of the lattice with a single dipole at the center of the cell does not always give the correct demagnetizing field [5].

It turns out that two-dimensional problems can be accurately and efficiently treated by the Fourier transform technique. In addition to calculating the demagnetizing fields within the film, this technique also allows the computation of magnetic fields outside the film. Thus, it can be applied to problems in other areas such as magnetic force microscopy [6] and simulation of readout from magnetic disk and tape. Energy considerations in the Fourier domain lead to significant insights as well as simplifications in certain micromagnetic problems. In this paper we outline the Fourier transform approach to magnetic field computation and present some preliminary results. More detailed computations and the results of dynamic simulations using the fast Fourier transform algorithm will be published elsewhere.

### The Field of a Long, Thin, Uniformly Magnetized Strip

Consider an infinitely long strip of height  $h$  and differential width  $dx$  located on the  $Y$  axis, as shown in Fig. 1. The strip has uniform magnetization  $\vec{M} = M_x \hat{x} + M_y \hat{y} + M_z \hat{z}$  and its field  $\vec{H}$  is to be calculated at an arbitrary point  $(x, y, z)$  in space. From symmetry it is clear that  $\vec{H}$  has no component in the  $Y$  direction and that the magnitudes of  $H_x$  and  $H_z$  are independent of the  $y$  coordinate of the observation point. One also observes that  $M_y$  does not contribute any field since the net magnetic charges created by  $M_y$  are finite in magnitude and located at infinity. The differential scalar potential  $d\phi(x, y, z)$  due to the uniform charge distributions on the four surfaces of the strip is calculated as follows:

$$d\phi(x, y, z) = \left[ 2M_x \left( \arctan \frac{z+\frac{h}{2}}{x} - \arctan \frac{z-\frac{h}{2}}{x} \right) + M_x \ln \left( \frac{x^2 + (z+\frac{h}{2})^2}{x^2 + (z-\frac{h}{2})^2} \right) \right] dx \quad (1)$$

Now, consider a film of thickness  $h$ , centered at  $Z = 0$  in the  $XY$  plane. Let the magnetization have a fixed direction in space with sinusoidal amplitude modulation along the  $X$  axis, namely,

$$\vec{M}(x, y, z) = \vec{M}_0 \exp(i2\pi f x) \quad (2)$$

where  $-\infty < x < \infty$ ,  $-\infty < y < \infty$ , and  $-\frac{h}{2} \leq z \leq \frac{h}{2}$ . Also assume that the spatial frequency  $f$  is greater than or equal to zero. The potential distribution will then be the convolution of the two functions in Eq.(1) and Eq.(2) and is given by:

$$\begin{aligned} \phi(x, y, z) = & -4\pi i \left[ (M_{x_0} - iM_{z_0}) \frac{\sinh(\pi h f)}{2\pi f} \exp(2\pi f z) \right] \exp(i2\pi f x); \quad z < -\frac{h}{2} \\ & -4\pi i \left[ -\frac{1}{2}(M_{x_0} - iM_{z_0}) \frac{\exp(2\pi f(z-\frac{h}{2}))}{2\pi f} - \frac{1}{2}(M_{x_0} + iM_{z_0}) \right. \\ & \quad \times \left. \frac{\exp(-2\pi f(z+\frac{h}{2}))}{2\pi f} + \frac{1}{2\pi f} M_{x_0} \right] \exp(i2\pi f x); \quad |z| \leq \frac{h}{2} \\ & -4\pi i \left[ (M_{x_0} + iM_{z_0}) \frac{\sinh(\pi h f)}{2\pi f} \exp(-2\pi f z) \right] \exp(i2\pi f x); \quad z \geq \frac{h}{2} \end{aligned} \quad (3)$$

The next step is to generalize the sinusoidal distribution of Eq.(2). Instead of running along the  $X$  axis, we let the sinusoid run along the arbitrary direction  $\hat{\sigma} = (f_x/f)\hat{x} + (f_y/f)\hat{y}$ . Here  $\hat{x}$  and  $\hat{y}$  are unit vectors along the  $X$  and  $Y$  axes,  $f_x$  and  $f_y$  are components of the spatial frequency, and  $f = \sqrt{f_x^2 + f_y^2}$  is the magnitude of the spatial frequency. The magnetization distribution is now given by

$$\vec{M}(x, y, z) = \vec{M}_0 \exp[i2\pi(f_x x + f_y y)] \quad (4)$$

The potential distribution can be obtained from Eq.(3) with the following modifications:

- i) Replace  $M_{x_0}$  with the component of  $\vec{M}_0$  along  $\hat{\sigma}$ , that is,  $\frac{f_x}{f} M_{x_0} + \frac{f_y}{f} M_{y_0}$
- ii) Replace  $\exp(i2\pi f x)$  with  $\exp[i2\pi(f_x x + f_y y)]$ .

Having found the potential distribution we obtain the magnetic field from the relationship  $\vec{H} = -\nabla\phi$ . Using the notation  $\hat{\sigma}_{\pm} = \frac{f_x}{f}\hat{x} + \frac{f_y}{f}\hat{y} \pm i\hat{z}$  where  $\hat{x}, \hat{y}, \hat{z}$  are Cartesian unit vectors and  $i = \sqrt{-1}$ , we find

$$\begin{aligned} \vec{H}(x, y, z) = & -4\pi \left[ \exp(2\pi f z) \sinh(\pi h f) (\vec{M}_0 \cdot \hat{\sigma}_-) \hat{\sigma}_- \right] \exp[i2\pi(f_x x + f_y y)]; \quad z < -\frac{h}{2} \\ & +4\pi \left[ \frac{1}{2} \exp[2\pi f(z - \frac{h}{2})] (\vec{M}_0 \cdot \hat{\sigma}_-) \hat{\sigma}_- + \frac{1}{2} \exp[-2\pi f(z + \frac{h}{2})] \right. \\ & \quad \left. (\vec{M}_0 \cdot \hat{\sigma}_+) \hat{\sigma}_+ - (\vec{M}_0 \cdot \hat{\sigma}) \hat{\sigma} \right] \exp[i2\pi(f_x x + f_y y)]; \quad |z| < \frac{h}{2} \\ & -4\pi \left[ \exp(-2\pi f z) \sinh(\pi h f) (\vec{M}_0 \cdot \hat{\sigma}_+) \hat{\sigma}_+ \right] \exp[i2\pi(f_x x + f_y y)]; \quad z > \frac{h}{2} \end{aligned} \quad (5)$$

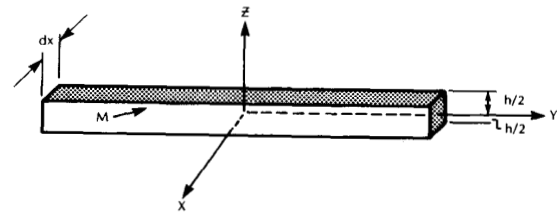


Figure 1: A long, thin strip of uniformly magnetized material.

In applications where the average field through the film thickness is desired, Eq.(5) yields:

$$\begin{aligned} \vec{H}_{\text{avg}}(x, y) = & \frac{1}{h} \int_{-\frac{h}{2}}^{+\frac{h}{2}} \vec{H}(x, y, z) dz = 4\pi \left\{ \exp(-\pi h f) \frac{\sinh(\pi h f)}{\pi h f} \right. \\ & \times \left[ \frac{1}{2}(\vec{M}_0 \cdot \hat{\sigma}_-) \hat{\sigma}_- + \frac{1}{2}(\vec{M}_0 \cdot \hat{\sigma}_+) \hat{\sigma}_+ \right] \\ & \left. - (\vec{M}_0 \cdot \hat{\sigma}) \hat{\sigma} \right\} \exp[i2\pi(f_x x + f_y y)] \end{aligned} \quad (6)$$

A comparison of the average field with the field at the center of the film (obtained from Eq.(5) by setting  $z = 0$ ) reveals the factor  $\frac{\sinh(\pi h f)}{\pi h f}$  in Eq.(6) as the only difference between the two expressions. The average field therefore has a stronger perpendicular component and a weaker in-plane component when compared to the field at the film center.

#### Field Calculation Using Fourier Transform

Consider a film of dimensions  $L_x, L_y$  and  $h$  where in the  $XYZ$  coordinate system  $0 \leq x \leq L_x$ ;  $0 \leq y \leq L_y$ ;  $-\frac{h}{2} \leq z \leq \frac{h}{2}$ . Let  $\vec{M}(x, y)$  be the magnetization of the film (uniform in the  $Z$  direction) and assume that periodic boundary conditions apply, namely, the  $XY$  plane is covered with identical  $L_x \times L_y$  tiles. The Fourier coefficients of the periodic function  $\vec{M}(x, y)$  are given by

$$\vec{M}_{mn} = \frac{1}{L_x L_y} \int_0^{L_x} \int_0^{L_y} \vec{M}(x, y) \exp[-i2\pi(\frac{mx}{L_x} + \frac{ny}{L_y})] dx dy \quad (7)$$

In Eq.(7) the  $x, y$ , and  $z$  components of  $\vec{M}$  are transformed separately. Now, the Fourier series representation of  $\vec{M}(x, y)$  is:

$$\vec{M}(x, y) = \sum_{m=-\infty}^{\infty} \sum_{n=-\infty}^{\infty} \vec{M}_{mn} \exp[i2\pi(\frac{mx}{L_x} + \frac{ny}{L_y})] \quad (8)$$

The field for each Fourier component of  $\vec{M}(x, y)$  is given in Eq.(5). (If the average field through the film thickness is desired one should use Eq.(6) instead.) Replacing  $f_x$  by  $m/L_x$ ,  $f_y$  by  $n/L_y$  and  $\vec{M}_0$  by  $\vec{M}_{mn}$ , one obtains the Fourier coefficients  $\vec{H}_{mn}$  of the field at constant  $z$ . The magnetic field distribution is then obtained by inverse Fourier transformation, namely,

$$\vec{H}(x, y, z) = \sum_{m=-\infty}^{\infty} \sum_{n=-\infty}^{\infty} \vec{H}_{mn}(z) \exp \left[ i2\pi \left( \frac{mx}{L_x} + \frac{ny}{L_y} \right) \right] \quad (9)$$

It is thus possible to obtain the average field or the field in a plane of constant  $z$  by a pair of Fourier transforms and some spatial filtering.

#### Energy Considerations

The magnetostatic energy density of the film discussed in the preceding section is

$$E_M = -\frac{1}{2L_x L_y} \int_0^{L_x} \int_0^{L_y} \vec{M}(x, y) \cdot \vec{H}_{\text{avg}}(x, y) dx dy \quad (10)$$

Using Parseval's theorem,  $E_M$  can be written in terms of the Fourier coefficients of  $\vec{M}$  and  $\vec{H}_{\text{avg}}$ , as follows:

$$\begin{aligned} E_M = & -\frac{1}{2} \sum_{n=-\infty}^{\infty} \sum_{m=-\infty}^{\infty} \vec{M}_{mn}^* \cdot \vec{H}_{mn} = 2\pi \sum_{n=-\infty}^{\infty} \sum_{m=-\infty}^{\infty} \left\{ \exp(-\pi h f) \right. \\ & \left. \frac{\sinh(\pi h f)}{\pi h f} [|\vec{M}_{mn} \cdot \hat{z}|^2 - |\vec{M}_{mn} \cdot \hat{\sigma}|^2] + |\vec{M}_{mn} \cdot \hat{\sigma}|^2 \right\} \end{aligned} \quad (11)$$

Another consequence of Parseval's theorem is the following relation between the average and the Fourier components of magnetization:

$$\langle M^2 \rangle = \frac{1}{L_x L_y} \int_0^{L_x} \int_0^{L_y} \vec{M} \cdot \vec{M}^* dx dy = \sum_{n=-\infty}^{\infty} \sum_{m=-\infty}^{\infty} |\vec{M}_{mn}|^2 \quad (12)$$

These equations allow the study of domain wall energies as related to the wall structure. We will discuss these issues in a separate publication.

#### Results and Discussion

Figure 2(a) shows the magnetization distribution for a reverse-magnetized circular domain in a perpendicularly magnetized medium. At each point on this discrete lattice of  $32 \times 32$  the perpendicular component of magnetization is represented by an arrow while the appendage to the arrow shows the in-plane component. In units of the lattice constant, the domain has radius  $R_0 = 8$  and wall thickness parameter  $\Delta_w = 3$ . The in-plane components of the wall have all been chosen to point in the same direction. (Although not the lowest energy state, this particular

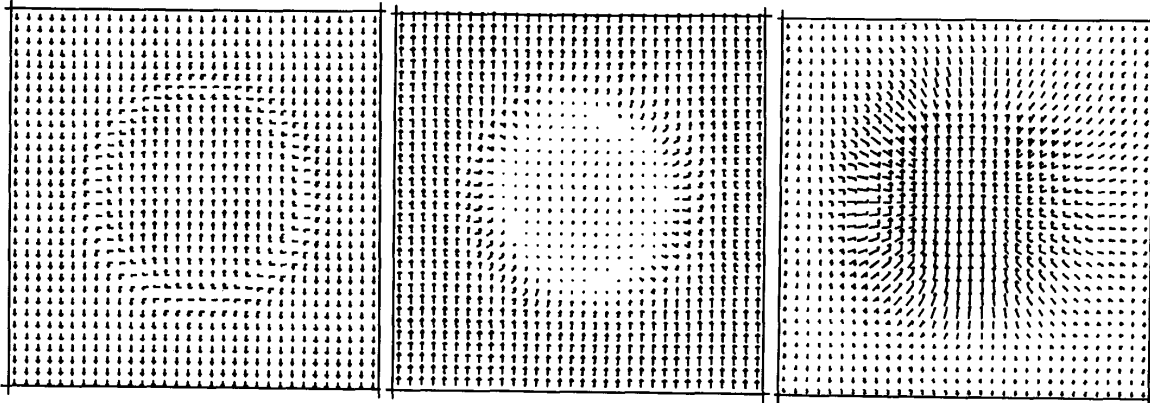


Figure 2(a): Magnetization distribution in a perpendicular film with a circular reverse domain. In units of the lattice constant the radius is  $R_0 = 8$  and the wall thickness parameter is  $\Delta_w = 3$ .

Figure 2(b): Thickness-averaged demagnetizing field for the magnetization distribution of Fig.2(a). In units of the lattice constant the film thickness is  $h = 10$ .

Figure 2(c): Magnetic field distribution outside the film of Fig.2(a) with  $h = 50$  at  $z = 26$ .

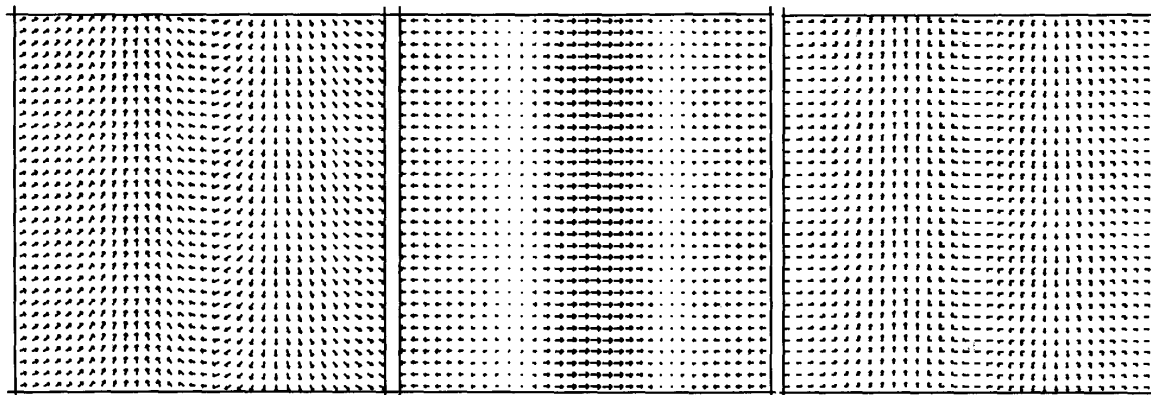


Figure 3(a): In-plane magnetization distribution with a pair of head-to-head walls.

Figure 3(b): Thickness-averaged demagnetizing field for the magnetization distribution of Fig. 3(a) with  $h = 10$ .

Figure 3(c): Magnetic field distribution outside the film of Fig. 3(a) with  $h = 10$  at  $z = 6$ .

choice exhibits some interesting features in its magnetic field distribution.) Figure 2(b) shows the thickness-averaged field  $\bar{H}_{avg}$ ; for this calculation the thickness  $h$  was 10 lattice constants. Notice the diminished magnitude of the demagnetizing field within the domain itself. At the same time, the charged walls on the right and the left give rise to strong in-plane fields while the contributions of the Bloch wall sections (above and below) to the field are insignificant. Figure 2(c) shows the field distribution outside the film. Here the film thickness is 50 and the field is calculated at a distance of one lattice constant above the film ( $z = 26$ ). Notice the slight asymmetry between the right and left halves of the picture in the area near the domain wall. This is due to the fact that the in-plane components of wall magnetization were chosen along the positive  $X$  axis, thereby creating asymmetry between the right and left half-domains. This asymmetry becomes even more pronounced for smaller film thicknesses.

Another example of demagnetizing field calculations using fast Fourier transforms is given in Fig. 3. Figure 3(a) shows the in-plane magnetization distribution for a film that contains two head-to-head walls. The average demagnetizing field  $\bar{H}_{avg}$  for a film thickness  $h = 10$  is shown in Fig. 3(b). The field outside the film at  $z = 6$  is shown in Fig. 3(c). The noteworthy feature of these results is that the field inside a head-to-head wall is very small while the demagnetizing energy is, of course, very large.

These preliminary results have shown that the computation of demagnetizing fields using fast Fourier transforms is far more accurate and efficient than the direct method of calculating dipole-dipole interactions. We are now in the process of incorporating this technique into our dynamic simulations and will report on the results in the near future.

#### Acknowledgement

This work has been made possible by a grant from the IBM Corporation.

#### References

- [1] C.C. Shir, "Computations of the Micromagnetic Dynamics in Domain Walls", *J. Appl. Phys.*, **49**, 3413-3421 (1978).
- [2] J.P. Peng and R.H. Victora, "Magnetic Recording Process Simulation", *IEEE Trans. Magn.*, **23**, 2865-2867 (1987).
- [3] J-G. Zhu and H.N. Bertram, "Micromagnetic Studies of Thin Metallic Films", *J. Appl. Phys.*, **63**, 3248-3253 (1988).

- [4] M. Mansuripur, "Magnetization Reversal Dynamics in the Media of Magneto-optical Recording", *J. Appl. Phys.*, **63**, 5809-5823 (1988).
- [5] M.E. Schabes and A. Aharoni, "Magnetostatic Interaction Fields for Three-dimensional Array of Ferromagnetic Cubes", *IEEE Trans. Magn.*, **23**, 3882-3888 (1987).
- [6] J.J. Sanez, and N. Garcia, "Observation of Magnetic Forces by the Atomic Force Microscope", *J. Appl. Phys.*, **62**, 4293-4295 (1987).